

Calcium-independent activation of endothelial nitric oxide synthase by ceramide

Junsuke Igarashi, Hemant S. Thatte, Prakash Prabhakar, David E. Golan, and Thomas Michel

PNAS 1999;96:12583-12588
doi:10.1073/pnas.96.22.12583

This information is current as of February 2007.

Online Information & Services	High-resolution figures, a citation map, links to PubMed and Google Scholar, etc., can be found at: www.pnas.org/cgi/content/full/96/22/12583
References	This article cites 29 articles, 17 of which you can access for free at: www.pnas.org/cgi/content/full/96/22/12583#BIBL This article has been cited by other articles: www.pnas.org/cgi/content/full/96/22/12583#otherarticles
E-mail Alerts	Receive free email alerts when new articles cite this article - sign up in the box at the top right corner of the article or click here .
Rights & Permissions	To reproduce this article in part (figures, tables) or in entirety, see: www.pnas.org/misc/rightperm.shtml
Reprints	To order reprints, see: www.pnas.org/misc/reprints.shtml

Notes:

Calcium-independent activation of endothelial nitric oxide synthase by ceramide

Junsuke Igarashi*[†], Hemant S. Thatte*^{‡§}, Prakash Prabhakar*, David E. Golan*^{§¶}, and Thomas Michel*^{||**}

Divisions of *Cardiology and [†]Hematology, Department of Medicine, Brigham and Women's Hospital, Boston, MA 02115; [‡]West Roxbury Veterans Affairs Medical Center, West Roxbury, MA 02132; and [§]Department of Biological Chemistry and Molecular Pharmacology, Harvard Medical School, Boston, MA 02115

Edited by Solomon H. Snyder, Johns Hopkins University School of Medicine, Baltimore, MD, and approved September 3, 1999 (received for review July 26, 1999)

The endothelial isoform of NO synthase (eNOS) is targeted to sphingolipid-enriched signal-transducing microdomains in the plasma membrane termed caveolae. Among the caveolae-targeted sphingolipids are the ceramides, a class of acylated sphingosine compounds that have been implicated in diverse cellular responses. We have explored the role of ceramide analogues in eNOS signaling in cultured bovine aortic endothelial cells (BAEC). Addition of the ceramide analogue *N*-acetyl sphingosine (C₂-ceramide; 5 μM) to intact BAEC leads to a significant increase in NO synthase activity (assayed by using the fluorescent indicator 4,5-diaminofluorescein) and translocation of eNOS from the endothelial cell membrane to intracellular sites (measured by using quantitative immunofluorescence techniques); the biologically inactive ceramide *N*-acetyldihydrosphingosine is entirely without effect. C₂-ceramide-induced eNOS activation and translocation are unaffected by the intracellular calcium chelator 1,2-bis-*o*-aminophenoxyethane-*N,N,N',N'*-tetraacetic acid (BAPTA). Using the calcium-specific fluorescent indicator fluo-3, we also found that C₂-ceramide activation of eNOS is unaccompanied by a drug-induced increase in intracellular calcium. These findings stand in sharp contrast to the mechanism by which bradykinin, estradiol, and other mediators acutely activate eNOS, in which a rapid, agonist-promoted increase in intracellular calcium is required. Finally, we show that treatment of BAEC with bradykinin causes a significant increase in cellular ceramide content; the response to bradykinin has an EC₅₀ of 3 nM and is blocked by the bradykinin B₂-receptor antagonist HOE140. Bradykinin-induced ceramide generation could represent a mechanism for longer-term regulation of eNOS activity. Our results suggest that ceramide functions independently of Ca²⁺-regulated pathways to promote activation and translocation of eNOS, and that this lipid mediator may represent a physiological regulator of eNOS in vascular endothelial cells.

The endothelial isoform of NO synthase (eNOS) is activated by diverse calcium-mobilizing agonists and by hemodynamic shear stress; the enzyme plays a key role in vascular homeostasis (see review in ref. 1). eNOS is targeted to specific microdomains in the plasma membrane termed caveolae, where the enzyme associates with the transmembrane scaffolding protein caveolin (reviewed in ref. 2). Caveolae serve as sites for the sequestration of many key signaling proteins in addition to eNOS, including G proteins, phospholipases, calmodulin, and diverse G protein-coupled receptors, including the bradykinin B₂ receptor (reviewed in ref. 3). At the ambient intracellular calcium concentrations ([Ca²⁺]_i) characteristic of resting cells, eNOS is tonically inhibited by its stable interaction with caveolin. Agonist- or flow-induced increases in [Ca²⁺]_i cause calmodulin to bind to and activate eNOS, in the process displacing caveolin from the enzyme (2, 4). Importantly, caveolae have a distinct lipid composition; these structures are highly enriched in sphingolipids and cholesterol and relatively depleted of phospholipids (5). Although this distinctive lipid milieu may function principally to generate a "liquid-ordered phase" for the structural organization of membrane domains (6), it seemed plausible to us that the

sphingolipids in caveolae could also serve signaling roles as lipid second messengers.

Ceramides are a class of sphingolipids formed by the acylation of sphingosine. This molecular class has been implicated broadly in cellular stress responses (see review in ref. 7). In several different cell types, specific cytokines have been found to promote marked increases in the content of cellular ceramide, which derives at least in part from precursors present in plasmalemmal caveolae (8). The cellular and molecular mechanisms that lead to receptor-mediated ceramide production are not well understood, although ceramide may be generated from sphingomyelin or glycosphingolipid precursors by the activation of sphingomyelinase (7) or glucocerebrosidase (9), respectively. Addition of specific ceramide analogues to cells appears to lead to apoptosis and other derangements in cell-cycle regulation and gene transcription; other closely related ceramide analogues are apparently without biological effect, indicating the existence of important structure-activity relationships in ceramide-regulated pathways (7). Diverse downstream events have been implicated in the disparate cellular roles of ceramide; protein kinase activation (7), receptor binding (10), allosteric effects (11), and protein translocation (12) have all been suggested as potential mechanisms mediating the cellular effects of this class of molecules. In at least some cellular systems, ceramide release may be potentiated by the addition of pharmacological sources of NO (13, 14). However, the high concentrations of NO-donating drugs that appear to be required for ceramide generation also lead to cellular apoptosis; these experimental systems are therefore unlikely to represent physiological signaling pathways.

It is not only the physical proximity of eNOS and sphingolipids in plasmalemmal caveolae that provides suggestive evidence for a regulatory connection. A recent report has described experiments in which the addition of a ceramide analogue to isolated blood vessels leads to vasorelaxation (15). It has also recently been shown that the G protein-coupled bradykinin B₂ receptor increases cellular ceramide content in cultured fibroblasts (16). In cultured endothelial cells, it has long been known that the same bradykinin B₂ receptor subtype activates eNOS (reviewed in ref. 17). Although purified eNOS is clearly a calmodulin-dependent enzyme (18, 19), studies in cultured endothelial cells

This paper was submitted directly (Track II) to the PNAS office.

Abbreviations: eNOS, endothelial isoform of NO synthase; BAEC, bovine aortic endothelial cells; DAGK, 1,2-diacyl-*sn*-glycerol kinase; BAPTA/AM, 1,2-bis-*o*-aminophenoxyethane-*N,N,N',N'*-tetraacetic acid tetra(acetoxymethyl) ester; DAF-2/DA, 4,5-diaminofluorescein diacetate; C₂-ceramide, *N*-acetyl sphingosine; C₂-dihydroceramide, *N*-acetyldihydrosphingosine; L-NNA, *N*^ω-nitro-L-arginine.

[†]J.I. and H.S.T. contributed equally to this work.

[¶]To whom reprint requests should be sent at the [†] address. E-mail: dgolan@hms.harvard.edu.

^{**}To whom reprint requests should be sent at the ^{*} address. E-mail: michel@calvin.bwh.harvard.edu.

The publication costs of this article were defrayed in part by page charge payment. This article must therefore be hereby marked "advertisement" in accordance with 18 U.S.C. §1734 solely to indicate this fact.

have not uniformly documented an absolute Ca^{2+} dependence for intracellular eNOS activation (20, 21). For example, bradykinin-dependent activation of eNOS is profoundly attenuated by chelation of intracellular calcium, yet the sustained increase in NO release induced by hemodynamic shear stress appears to be largely independent of $[\text{Ca}^{2+}]_i$ increases (20). In the present studies, we demonstrate that ceramide can promote eNOS activation and enzyme translocation in endothelial cells. Importantly, the effects of ceramide on the regulation of eNOS are entirely unaffected by chelation of intracellular calcium, providing a possible explanation for the variable Ca^{2+} dependency of cellular NO synthesis in different experimental settings.

Methods

Materials. FBS was from HyClone; all other cell culture reagents and media were from Life Technologies (Rockville, MD). Bovine heart cardiolipin and brain ceramide were from Avanti Polar Lipids. 1,2-Diacyl-*sn*-glycerol kinase (DAGK), 1,2-bis-*o*-aminophenoxyethane-*N,N,N',N'*-tetraacetic acid tetra(acetoxymethyl) ester (BAPTA/AM), and 4,5-diaminofluorescein diacetate (DAF-2/DA) were from Calbiochem. *N*-Acetylsphingosine (C_2 -ceramide) and *N*-acetyldihydrosphingosine (C_2 -dihydroceramide) were from Biomol (Plymouth Meeting, PA), and $[\gamma\text{-}^{32}\text{P}]\text{ATP}$ was from ICN. Protein determinations used the Bio-Rad protein assay kit with gamma globulin as standard. Fluo-3 was from Molecular Probes. The bradykinin receptor antagonist HOE140 was from Research Biochemicals (Natick, MA). Anti-eNOS mAb was from Transduction Laboratories (Lexington, KY). Other reagents were from Sigma.

Cell Culture and Drug Treatment. Bovine aortic endothelial cells (BAEC) were from Cell Systems (Kirkland, WA) and maintained in culture as described (22). For ceramide measurement, cells were plated onto gelatin-coated 6-well plates and studied prior to cell confluence at passage 5–7. For immunostaining experiments, cells were plated onto gelatin-coated glass coverslips and processed exactly as previously reported (23, 24). All drug treatments were carried out in complete medium; control cultures were incubated in parallel with vehicle-containing medium. Stock solutions of C_2 -ceramide and C_2 -dihydroceramide were prepared in ethanol and stored at -20°C .

Immunolabeling of eNOS Protein. The subcellular localization of eNOS protein in BAEC was evaluated with quantitative cell imaging, as recently described in detail (23, 24). Briefly, endothelial cells were fixed and permeabilized, then stained with an anti-eNOS mAb, followed by a rhodamine-conjugated goat anti-mouse IgG Ab. Cells were analyzed with a Zeiss epifluorescence microscope equipped with differential interference contrast optics. At least 100 cells on each coverslip were evaluated for eNOS staining at the cell membrane by an examiner who had been blinded to the culture conditions. The proportion of cells exhibiting eNOS staining at the cell membrane was quantitated for each experimental treatment, normalized to the fraction of eNOS “membrane-positive cells” present in the control culture for each experiment, and analyzed as described previously (23, 24). Each experiment was performed three to five times in duplicate.

Quantitation of Intracellular NO Generation. NO production in intact BAEC was measured with the recently described fluorescent indicator DAF-2 (25, 26). BAEC were plated onto gelatin-coated glass coverslips and incubated with the membrane-permeant diacetate form of DAF-2 in DMEM for 1 h at 37°C , in the presence or absence of the NO synthase inhibitor *N*^ω-nitro-L-arginine (L-NNA; final concentration, $100\ \mu\text{M}$). In some cultures, BAPTA/AM (final concentration, $20\ \mu\text{M}$) was added during the last 20 min of the incubation with DAF-2/DA. After

the cells had been washed with DMEM, the coverslip bearing the cells was mounted on a custom-made microscopy chamber that allowed rapid exchange of medium without disturbing the cells. Cells were then analyzed by using an epifluorescence microscope with a cooled charge-coupled device camera, and DAF-2 fluorescence counts were recorded in real time before and after drug treatment, as recently described (24). Typically, 5–10 cells were identified in a field of view at $25\times$ magnification, and changes in the integrated fluorescence intensity of each cell were monitored over time. Cell boundaries were drawn by using an image processor (MetaMorph; Universal Imaging, Media, PA), and fluorescence intensity was integrated over all pixels within the boundary of each individual cell. The fluorescence intensities within each experiment were normalized to a reference image recorded before drug treatment. The data shown are from studies performed in duplicate and repeated at least three times.

Determination of $[\text{Ca}^{2+}]_i$. $[\text{Ca}^{2+}]_i$ was determined by using the indicator dye fluo-3, as described (23, 24). Briefly, BAEC were plated onto gelatin-coated glass coverslips and incubated with fluo-3/AM in Hanks' balanced salt solution for 1 h at room temperature, then analyzed with epifluorescence microscopy before and after drug treatment. The experiments were performed in duplicate and repeated three times.

Ceramide Measurement. BAEC were washed with ice-cold PBS (Dulbecco's formulation), then scraped into $300\ \mu\text{l}$ of ice-cold balanced salt solution (BSS; described in ref. 27). The harvested cells were sonicated, and $100\ \mu\text{l}$ of the lysate was removed to a glass tube. Cellular lipids were isolated by using chloroform/methanol as described (28), then stored under nitrogen at -20°C and analyzed within 72 h. Ceramide content was quantified after *in vitro* conversion of ceramide to ceramide 1- $[\text{P}^{32}]\text{phosphate}$ with the DAGK reaction, essentially as described (29). Cellular lipids were dried under nitrogen, then solubilized into $20\ \mu\text{l}$ of buffer containing 5 mM cardiolipin and 7.5% (vol/vol) *n*-octyl β -D-glucopyranoside in 1 mM diethylenetriamine pentaacetic acid (DETAPAC; pH 7.0), then added (on ice) to $50\ \mu\text{l}$ of reaction

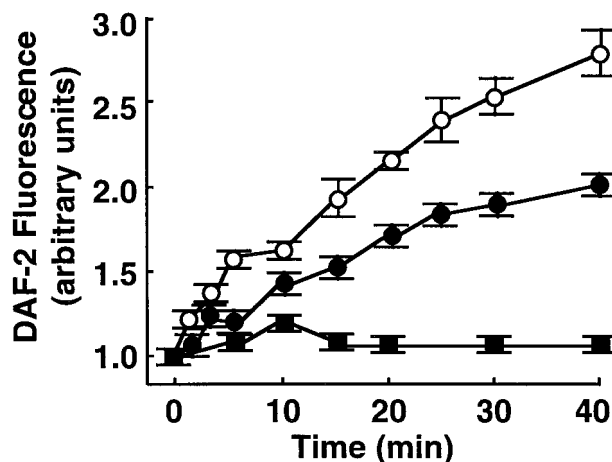


Fig. 1. Effects of C_2 -ceramide on NO production in endothelial cells. BAEC were incubated with the NO indicator dye DAF-2/DA and processed for intracellular NO generation as described in the text. The integrated fluorescence intensity was measured over time after treatment of the cells with C_2 -ceramide ($5\ \mu\text{M}$) in the presence or absence of L-NNA ($100\ \mu\text{M}$) and normalized to the fluorescence intensity measured before drug treatment. A total of 20–25 cells in three independent culture preparations were examined; each data point represents the mean \pm SE, and the slopes of the lines differ significantly from one another at the $P < 0.0001$ level. ●, Vehicle-treated cells; ○, C_2 -ceramide alone; ■, C_2 -ceramide plus L-NNA.

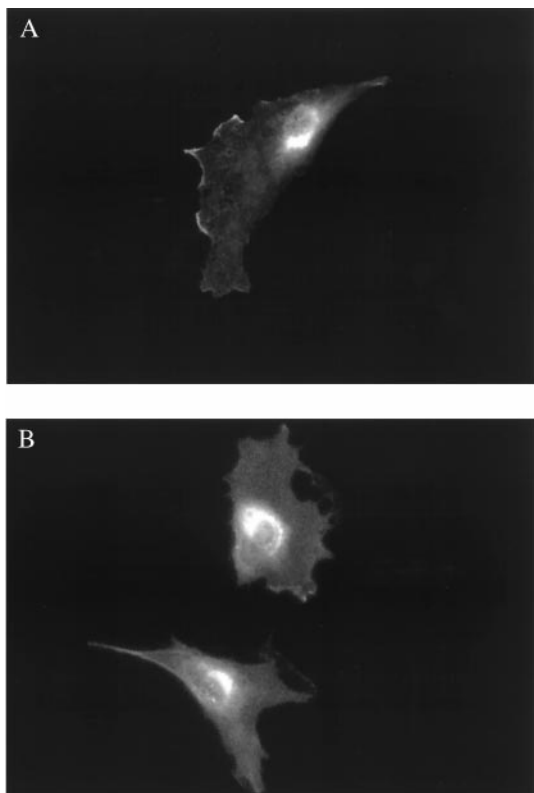


Fig. 2. Translocation of eNOS in endothelial cells in response to C_2 -ceramide. Shown are typical photomicrographs of BAEC processed for immunofluorescence as described in the text. (A) A representative image of eNOS-immunolabeled endothelial cells studied under basal conditions. (B) A representative image after treatment of endothelial cells with C_2 -ceramide ($5 \mu\text{M}$) for 30 min. Both images are shown at $250\times$ magnification and printed with identical brightness and contrast settings.

mixture (29), $14.5 \mu\text{l}$ of H_2O , $2 \mu\text{l}$ of 20 mM DTT in 1 mM DETAPAC (pH 7.0), and $3.5 \mu\text{l}$ of high-purity recombinant bacterial DAGK (enzyme activity >12 units/mg protein). The enzyme reaction was started by adding $10 \mu\text{l}$ of 10 mM ATP containing $[\gamma\text{-}^{32}\text{P}]\text{ATP}$ (specific activity, ≈ 100 dpm/pmol of ATP) in 1 mM DETAPAC (pH 7.0). After incubation at 37°C for 1 h, the reaction was terminated by adding 3 ml of chloroform/methanol (1:2, vol/vol) and 0.7 ml of 1% HClO_4 (vol/vol) and vortexing, and the mixture was then extracted with 2 ml of chloroform/1% HClO_4 (1:1, vol/vol). The upper phase was discarded; the lower phase was dried under nitrogen and solubilized in $30 \mu\text{l}$ of chloroform/methanol (95:5, vol/vol). The samples containing ceramide 1- ^{32}P phosphate were applied to a Whatman LK6D TLC plate and developed with a solvent system comprising chloroform/methanol/acetic acid (65:15:5 by volume). After air-drying, the TLC plate was subjected to autoradiography on X-Omat film (typically ≈ 18 h) and then to densitometric analysis with a ChemImager 4000 (Alpha Innotech, San Leandro, CA). Ceramide content was quantified within each experiment by using a standard curve established by assaying samples of authentic brain ceramide (50–400 pmol) processed and analyzed in parallel; the reference ceramide yielded an R_f value of 0.25, as reported (27). In different experiments, the quantity of ceramide in a given well of untreated BAEC ranged from 150 to 300 pmol (1.8 ± 0.2 nmol of ceramide/mg of cellular protein; mean \pm SE, $n = 6$). Within each experiment, the quantity of cellular ceramide after drug treatment was normalized to the ceramide content in the control culture, determined in duplicate.

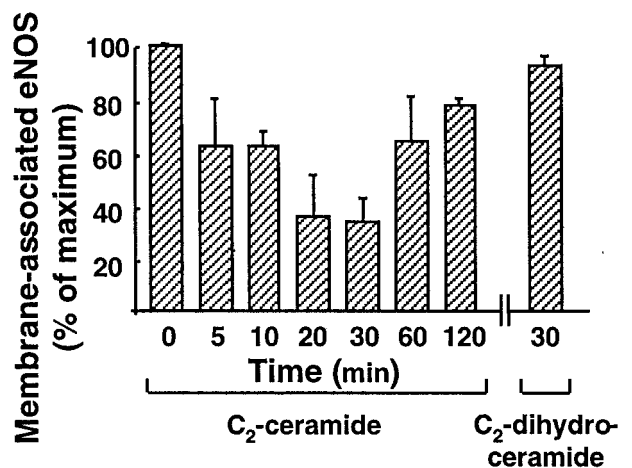


Fig. 3. Time course of C_2 -ceramide-induced eNOS translocation. BAEC were treated with C_2 -ceramide ($5 \mu\text{M}$) or with C_2 -dihydroceramide ($5 \mu\text{M}$) for the times indicated. The proportion of cells with eNOS immunoreactivity at the cell membrane was determined as described in *Methods* and as previously reported (23, 24); the basal value (at $t = 0$) was used to normalize the percentage of cells with eNOS membrane-positive staining at each subsequent time point. At each time point, 100–120 cells were scored; the data shown represent the mean \pm SE derived from three independent culture preparations.

Results

BAEC were treated with the cell-permeant ceramide, C_2 -ceramide (30); the biologically inactive analogue C_2 -dihydroceramide (30) was used as a negative control. We first studied the effects of C_2 -ceramide on NO production in intact BAEC by using the NO-specific fluorescent indicator DAF-2, which reacts covalently with NO to yield the brightly fluorescent triazolofluorescein (24–26). Using quantitative fluorescence microscopy to monitor DAF-2 fluorescence over time, we found a tonic level of NO synthesis in BAEC that was attenuated by the NO synthase inhibitor L-NNA (Fig. 1). The addition of C_2 -ceramide ($5 \mu\text{M}$) markedly stimulated cellular NO synthesis relative to that in untreated BAEC; the stimulatory effects of C_2 -ceramide were completely blocked by L-NNA (Fig. 1). The inactive analogue C_2 -dihydroceramide did not stimulate NO synthesis (data not shown).

We have previously used immunofluorescence approaches to show that bradykinin and estradiol induce the translocation of eNOS protein from the plasma membrane to intracellular sites (23, 24). Here, we used similar approaches to study the effects of ceramide on eNOS translocation. Most resting endothelial cells showed eNOS staining at the plasma membrane as well as at intracellular sites (Fig. 2A; see refs. 23, 24). Treatment of endothelial cells with C_2 -ceramide ($5 \mu\text{M}$, 30 min) caused the proportion of BAEC with plasma membrane-associated eNOS to decrease markedly and eNOS protein to translocate to intracellular sites (Fig. 2B). These findings are similar to those observed after bradykinin (23) or estradiol (24) treatment of endothelial cells. Importantly, the biologically inactive C_2 -dihydroceramide (30) failed to alter the pattern of eNOS staining (Fig. 3). We used quantitative immunofluorescence approaches (23, 24) to analyze the time course of ceramide-induced eNOS translocation (Fig. 3). The fraction of endothelial cells showing eNOS staining at the cell membrane began to decline 5 min after the addition of C_2 -ceramide to BAEC, reaching a minimal value at 30 min and then gradually returning to basal values at 120 min. In contrast, C_2 -dihydroceramide had no effect on the subcellular distribution of eNOS at any time point (Fig. 3).

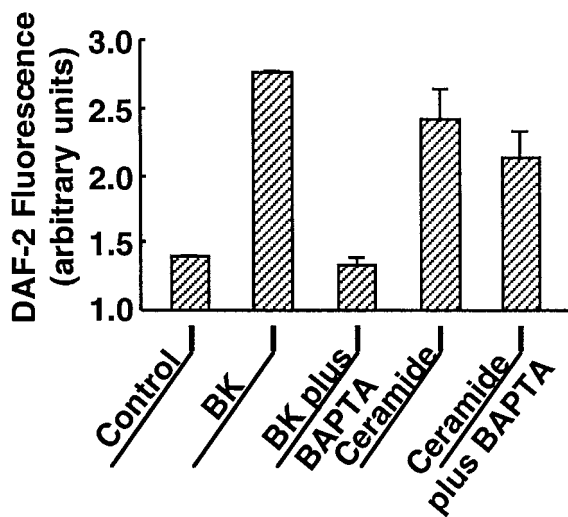


Fig. 4. Effects of intracellular calcium chelation by BAPTA on C_2 -ceramide- vs. bradykinin-activated NO production. BAEC were incubated with the NO indicator dye DAF-2/DA and processed for intracellular NO generation as described in the text. The integrated fluorescence intensity was measured before and 15 min after addition of bradykinin ($1 \mu\text{M}$) or C_2 -ceramide ($5 \mu\text{M}$); data shown are normalized to the fluorescence intensity measured prior to drug addition. As indicated in the figure, some cultures were incubated in the presence of the intracellular calcium chelator BAPTA/AM ($20 \mu\text{M}$ for 20 min) prior to addition of bradykinin (BK) or C_2 -ceramide. For each treatment, 20–25 cells in three independent culture preparations were examined; each data point represents the mean \pm SE.

We have previously reported that agonist-dependent eNOS activation and translocation can be completely abrogated by the intracellular calcium chelator BAPTA (23, 24). We therefore explored the effects of BAPTA on eNOS activation by ceramide. As shown in Fig. 4, the calcium chelator had no effect on the robust activation of eNOS by C_2 -ceramide ($5 \mu\text{M}$), whereas the effect of bradykinin was completely blocked. These data indicate that exogenous ceramide induces NO production in endothelial cells in a calcium-independent manner. In a similar fashion, chelation of intracellular calcium by BAPTA failed to block ceramide-induced eNOS translocation, although bradykinin-induced eNOS translocation was abrogated by BAPTA (Fig. 5). Taken together, these data suggest that eNOS activation and translocation by C_2 -ceramide do not require the mobilization of intracellular calcium. We then used the calcium-specific fluorescent indicator fluo-3 to determine whether C_2 -ceramide itself directly elevates $[\text{Ca}^{2+}]_i$ (Fig. 6). Treatment of fluo-3-loaded BAEC with C_2 -ceramide elicited no increase in $[\text{Ca}^{2+}]_i$, whereas the calcium ionophore A23187 was still capable of increasing $[\text{Ca}^{2+}]_i$ in cells pretreated with C_2 -ceramide, indicating that neither intracellular calcium mobilization nor the fluorescence properties of fluo-3 were attenuated by ceramide under these experimental conditions.

Finally, we examined the effect of bradykinin on the ceramide content of endothelial cells. Treatment of BAEC with bradykinin ($10 \mu\text{M}$) caused a \approx 2-fold increase in cellular ceramide content relative to control (untreated) cells (Fig. 7A). The ceramide content in resting BAEC was $1.8 \pm 0.2 \text{ nmol/mg}$ of protein (mean \pm SE, $n = 6$); ceramide content reached a maximum value at 3 min ($4.3 \pm 0.8 \text{ nmol/mg}$ protein, $n = 6$; $P < 0.05$ vs. control cells by ANOVA), then decreased to the basal level by 12 min after drug addition. The dose-dependence of the bradykinin-stimulated ceramide response was studied at 3 min after drug treatment, and is shown in Fig. 7B. A significant bradykinin-induced increase in BAEC ceramide content was apparent at 1 nM drug and was maximal at $1 \mu\text{M}$; the EC_{50} was

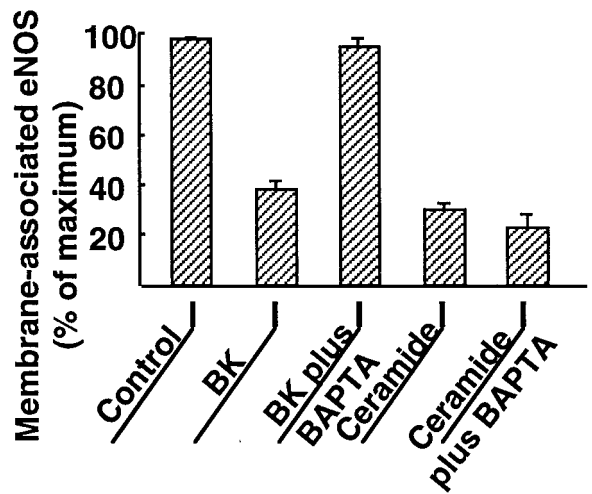


Fig. 5. Effects of intracellular calcium chelation by BAPTA on C_2 -ceramide- vs. bradykinin-activated eNOS translocation. BAEC that had been incubated with or without BAPTA/AM ($20 \mu\text{M}$ for 20 min) were then treated with bradykinin (BK; $1 \mu\text{M}$ for 5 min) or C_2 -ceramide ($5 \mu\text{M}$ for 30 min), as indicated in the figure, and then processed and analyzed for eNOS membrane-positive immunostaining as described in the text. Each data point represents the mean \pm SE derived from analysis of 100–120 cells per treatment in three independent culture preparations.

3 nM. The bradykinin B_2 -receptor antagonist HOE140 (31) completely abrogated the bradykinin-induced ceramide increase (Fig. 7B). HOE140 by itself was without effect; the ceramide content in BAEC 3 min after HOE140 treatment was $99.0 \pm 17.4\%$ relative to vehicle control (mean \pm SE, $n = 4$). These data indicate that bradykinin, in addition to its extensively characterized role as an agonist for the Ca^{2+} -dependent activation of eNOS, also transiently elevates endogenous ceramide levels in endothelial cells.

Discussion

The present study provides evidence that specific ceramides could have an important impact on the eNOS signaling pathway.

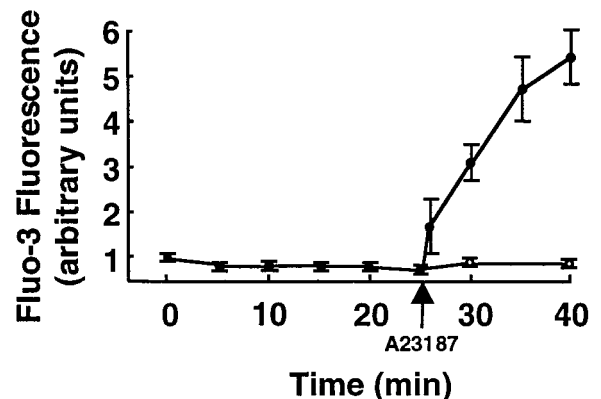


Fig. 6. Effects of C_2 -ceramide on $[\text{Ca}^{2+}]_i$ in endothelial cells. BAEC were incubated with the calcium indicator fluo-3/AM and processed for $[\text{Ca}^{2+}]_i$ measurements, as described in the text. The integrated fluo-3 fluorescence intensity of each cell was measured in real time before and after treatment with either C_2 -ceramide alone ($5 \mu\text{M}$, ○) or C_2 -ceramide ($5 \mu\text{M}$ for 25 min) followed by A23187 ($10 \mu\text{M}$, ●). The data were normalized to the fluorescence intensity measured before the addition of C_2 -ceramide. A total of 20–25 cells were analyzed for each treatment; each data point represents the mean \pm SE from three independent culture preparations.

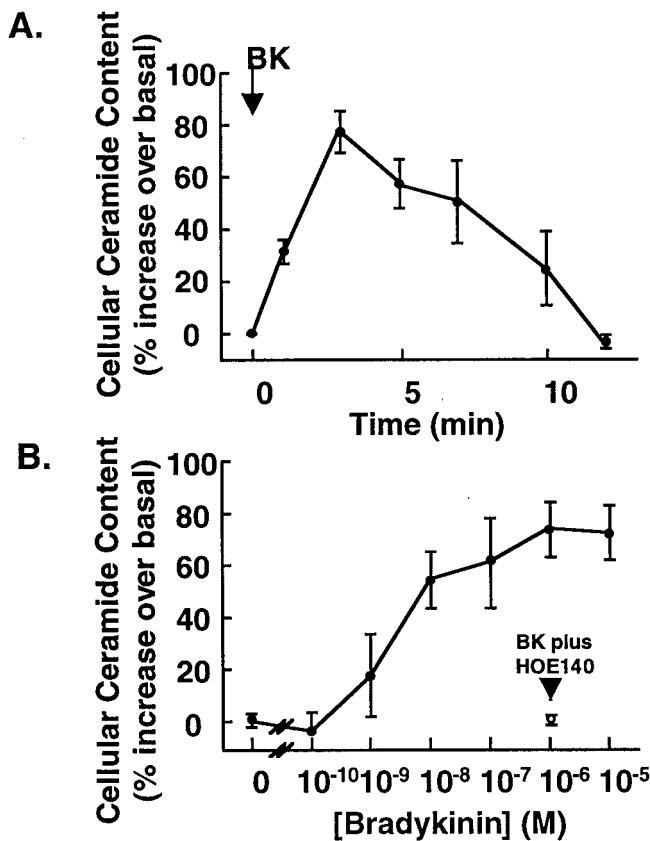


Fig. 7. Ceramide generation by bradykinin in BAEC. BAEC were treated with bradykinin, then processed for quantitation of cellular ceramide content. (A) Time course of ceramide generation by bradykinin. After addition of bradykinin (10 μ M), endothelial cells grown in six-well dishes were harvested at the indicated times, and cellular ceramide content was quantified as described in *Methods*. The relative increase over basal cellular ceramide content (which ranged from 150 to 300 pmol per well) was calculated at each time point; each data point represents the mean \pm SE derived from six independent culture preparations, each performed in duplicate. (B) Dose dependence of ceramide generation by bradykinin. Endothelial cells were treated with the indicated concentrations of bradykinin for 3 min, then harvested and processed for ceramide content. The cellular ceramide content at each dose was normalized relative to the basal value determined for vehicle-treated cells within each experiment; each data point represents the mean \pm SE derived from five independent culture preparations, each analyzed in duplicate. The single data point with the open circle shows the relative ceramide content in cells treated with bradykinin (1 μ M) plus the bradykinin B₂-receptor antagonist HOE140 (3 μ M).

To characterize the direct effects of ceramide, we have studied the cellular responses to the cell-permeant ceramide analogue *N*-acetyl sphingosine (*C*₂-ceramide). This agent has previously been applied in studies of ceramide effects on cell-cycle regulation and apoptosis (7, 30). The closely related analogue *C*₂-dihydroceramide, which differs from the active compound solely by the reduction of one double bond in the ceramide's alkyl side chain, is without biological effects in these systems (30). Addition of *C*₂-ceramide, but not *C*₂-dihydroceramide, leads to the robust activation of NO synthesis in endothelial cells (Figs. 1 and 4). As seen previously for bradykinin (23), *C*₂-ceramide also promotes the reversible translocation of eNOS from plasma membrane to intracellular sites (Figs. 2, 3, and 5). However, in marked contrast to the effects of bradykinin, the effects of ceramide on eNOS activation and translocation appear to proceed by a calcium-independent pathway. As we have previously shown (23, 24), and as reproduced in the present study (Figs. 4

and 5), chelation of intracellular calcium with BAPTA abrogates receptor-mediated eNOS activation and translocation in endothelial cells. In contrast, the effects of ceramide on eNOS activation and translocation are not affected by BAPTA (Figs. 4 and 5), and ceramide itself does not appear to increase intracellular Ca²⁺ levels (Fig. 6).

As eNOS is a Ca²⁺/calmodulin-dependent enzyme, how could ceramide activate eNOS without a detectable increase in [Ca²⁺]_i? The different NOS isoforms are known to differ markedly in their Ca²⁺ requirements for full enzyme activation by calmodulin. For example, the inducible NOS (iNOS) isoform effectively contains calmodulin as a subunit, in that the enzyme binds calmodulin tightly, even at the low [Ca²⁺]_i characteristic of resting cells (19). In contrast, eNOS and neuronal NOS are transiently activated by the elevations in [Ca²⁺]_i that follow receptor activation. The rapid response of endothelial cells to ceramide is incompatible with the *de novo* induction of iNOS. It is possible that structural characteristics of the eNOS protein are transiently modulated so as to alter the enzyme's Ca²⁺ dependency for activation by calmodulin. This effect could be achieved, for example, by direct binding of ceramide to eNOS, or by ceramide-activated phosphorylation pathways. Interestingly, Venema *et al.* (32) have shown that eNOS can be potently inhibited by acidic phospholipids, and sphingolipids have been documented both to increase (33) and decrease (34, 35) [Ca²⁺]_i levels. It is also possible that ceramide stimulates localized increases in [Ca²⁺]_i levels that are below the limits of detection of the methods used in this study.

The nonapeptide bradykinin represents an important physiological activator of eNOS in the vascular endothelium, promoting rapid and transient Ca²⁺-dependent activation of the enzyme. More prolonged bradykinin stimulation induces eNOS to translocate from plasmalemmal caveolae to intracellular sites, from which the enzyme eventually returns to the cell membrane (23). As shown in Fig. 7, treatment of BAEC with bradykinin causes an \approx 2-fold increase in cellular ceramide content within 3 min, and the ceramide content decreases to baseline levels within 12 min of incubation. This response to bradykinin has an EC₅₀ of 3 nM and is completely blocked by the B₂-receptor antagonist HOE140, indicating the involvement of the bradykinin B₂ receptor (Fig. 7). The signaling responses elicited by endothelial cell B₂-receptor activation are multiple and complex (17), including phosphorylation of the B₂ receptor itself, activation of G proteins, activation of phospholipase C with downstream mobilization of intracellular Ca²⁺, phosphorylation of numerous serine and tyrosine residues on intracellular proteins, and activation of eNOS. These and other signaling pathways initiated by bradykinin are likely to lead to complex interdependent downstream responses in endothelial cells. Although bradykinin both activates eNOS and increases cellular ceramide content, it would be misleading to conclude from our data that ceramide generation is an obligate intermediate in bradykinin's rapid Ca²⁺-dependent activation of eNOS. It seems more plausible that bradykinin's well characterized Ca²⁺-dependent activation of eNOS involves a separate proximal signaling pathway that is distinct from the Ca²⁺-independent process of ceramide generation. Indeed, the time course for *C*₂-ceramide-induced translocation of eNOS is slower than that seen in response to bradykinin. This delayed response could reflect solely the time required for extracellular ceramide to reach its intracellular targets, but it could also be the case that ceramide generation represents a mechanism for the longer-term regulation of eNOS activity. Previous studies have identified important differences in the time course and calcium sensitivity of receptor- vs. shear stress-mediated activation of eNOS (20). It will be important to extend the present observations to the analysis of eNOS activation by shear stress.

Numerous pathways that could lead to receptor-coupled ceramide generation have been postulated in other cellular systems, but the detailed mechanisms are not well understood. The colocalization of receptors for extracellular signals, potential lipid precursors of ceramide, and eNOS within endothelial plasmalemmal caveolae is notable, suggesting that the caveolae microdomain could serve to sequester these and other signaling molecules to facilitate their rapid activation following receptor activation. In some cell types, the activation of sphingomyelinase by cytokines appears to lead to a robust and sustained generation of ceramide followed by cellular apoptosis (7); the mechanism responsible for sphingomyelinase activation remains to be elucidated. A recent study suggests that bradykinin can induce the degradation of glycosphingolipid in fibroblasts without activating sphingomyelinase (16). In an analogous fashion, activation of a glucocerebrosidase could modulate the receptor-induced generation of ceramide in endothelial cells by converting glucosylceramide to ceramide. Another potential pathway could involve the activation of EDG-1, a G-protein-coupled receptor expressed in endothelial cells that is activated by sphingosine 1-phosphate (10); ceramide and/or related sphingolipid derivatives could regulate eNOS signaling through interactions with EDG-1. At this point, however, the specific sphingolipid species

from which ceramide is generated, the enzyme(s) that generate ceramide after receptor activation, and the proximal signals that activate the enzyme all remain to be elucidated.

The current studies have provided several lines of evidence documenting a role for ceramide in eNOS regulation. The distinct lipid composition of plasmalemmal caveolae could importantly influence the spatial relationships between signaling proteins and markedly affect the physical milieu in which these proteins interact. The current studies suggest that the enrichment of caveolae in specific sphingolipids could serve also to facilitate eNOS regulation in endothelial cells. The interrelationships between receptor agonists and ceramide lipid mediators in the regulation of the activity and subcellular distribution of eNOS could provide another point of control for NO-dependent signaling in the vascular wall.

This work was supported by awards from the National Institutes of Health (to T.M. and D.E.G.) and from the American Heart Association and the Burroughs Wellcome Fund (to T.M.). J.I. is a recipient of postdoctoral fellowships from the Japan Heart Foundation and the Yamanouchi Foundation for Research on Metabolic Diseases. P.P. is supported by a fellowship from the Brigham and Women's Hospital Research Organization. T.M. is a Burroughs Wellcome Scholar in Experimental Therapeutics.

1. Welch, G. & Loscalzo, J. (1995) *Prog. Cardiovasc. Dis.* **38**, 87–104.
2. Michel, T. & Feron, O. (1997) *J. Clin. Invest.* **100**, 2146–2152.
3. Shaul, P. W. & Anderson, R. G. W. (1998) *Am. J. Physiol.* **275**, L843–L851.
4. Feron, O., Saldana, F., Michel, J. B. & Michel, T. (1998) *J. Biol. Chem.* **273**, 3125–3128.
5. Brown, D. A. & Rose, J. K. (1992) *Cell* **68**, 533–544.
6. Brown, D. A. & London, E. (1997) *Biochem. Biophys. Res. Commun.* **240**, 1–7.
7. Hannun, Y. A. (1996) *Science* **274**, 1855–1859.
8. Liu, P. & Anderson, R. G. W. (1995) *J. Biol. Chem.* **270**, 27179–27185.
9. Prenc, E. M. (1995) *Biochem. J.* **310**, 571–575.
10. Lee, M. J., Van Brocklyn, J. R., Thangada, S., Liu, C. H., Hand, A. R., Menzeleev, R., Spiegel, S. & Hla, T. (1998) *Science* **279**, 1552–1555.
11. Bhat, B. G., Wang, P. & Coleman, R. A. (1995) *Biochemistry* **34**, 11237–11244.
12. Sawai, H., Okazaki, T., Takeda, Y., Tashima, M., Sawada, H., Okuma, M., Kishi, S., Umehara, H. & Domae, N. (1997) *J. Biol. Chem.* **272**, 2452–2458.
13. Huwiler, A., Pfeilschifter, J. & van den Bosch, H. (1999) *J. Biol. Chem.* **274**, 7190–7195.
14. Takeda, Y., Tashima, M., Takahashi, A., Uchiyama, T. & Okazaki, T. (1999) *J. Biol. Chem.* **274**, 10654–10660.
15. Johns, D. G., Jin, J. S. & Webb, R. C. (1998) *Eur. J. Pharmacol.* **349**, 9–10.
16. Meacci, E., Vasta, V., Farnararo, M. & Bruni, P. (1996) *Biochem. Biophys. Res. Commun.* **221**, 1–7.
17. Mombouli, J. & Vanhoutte, P. (1995) *Annu. Rev. Pharmacol. Toxicol.* **35**, 679–705.
18. Marletta, M. A. (1994) *Cell* **78**, 927–930.
19. Nathan, C. & Xie, Q. W. (1994) *Cell* **78**, 915–918.
20. Kuchan, M. J. & Frangos, J. A. (1994) *Am. J. Physiol.* **266**, C628–C636.
21. Fleming, I., Bauersachs, J., Fisslthaler, B. & Busse, R. (1998) *Circ. Res.* **82**, 686–695.
22. Michel, T., Li, G. K. & Busconi, L. (1993) *Proc. Natl. Acad. Sci. USA* **90**, 6252–6256.
23. Prabhakar, P., Thatte, H. S., Goetz, R. M., Cho, M. R., Golan, D. E. & Michel, T. (1998) *J. Biol. Chem.* **273**, 27383–27388.
24. Goetz, R. M., Thatte, H. S., Prabhakar, P., Cho, M. R., Michel, T. & Golan, D. E. (1999) *Proc. Natl. Acad. Sci. USA* **97**, 2788–2793.
25. Kojima, H., Sakurai, K., Kikuchi, K., Kawahara, S., Kirino, Y., Nagoshi, H., Hirata, Y. & Nagano, T. (1998) *Chem. Pharm. Bull.* **46**, 373–375.
26. Nakatsubo, N., Kojima, H., Kikuchi, K., Nagoshi, H., Hirata, Y., Maeda, D., Imai, Y., Irimura, T. & Nagano, T. (1998) *FEBS Lett.* **427**, 263–266.
27. Younes, A., Kahn, D. W., Besterman, J. M., Bittman, R., Byun, H. S. & Kolesnick, R. N. (1992) *J. Biol. Chem.* **267**, 842–847.
28. Bligh, E. A. & Dyer, W. J. (1959) *Can. J. Biochem. Physiol.* **37**, 911–917.
29. Preiss, J. E., Loomis, C. R., Bell, R. M. & Niedel, J. E. (1987) *Methods Enzymol.* **141**, 294–300.
30. Verheij, M., Bose, R., Lin, X. H., Yao, B., Jarvis, W. D., Grant, S., Birrer, M. J., Szabo, E., Zon, L. I., Kyriakis, J. M., et al. (1996) *Nature (London)* **380**, 75–79.
31. Hock, F. J., Wirth, K., Albus, U., Linz, W., Gerhards, H. J., Wiemer, G., Henke, S., Breipohl, G., Konig, W., Knolle, J. & Scholkens, B. A. (1991) *Br. J. Pharmacol.* **102**, 769–773.
32. Venema, R. C., Sayegh, H. S., Arnal, J. F. & Harrison, D. G. (1995) *J. Biol. Chem.* **270**, 14705–14711.
33. Mao, C., Kim, S. H., Almenoff, J. S., Rudner, X. L., Kearney, D. M. & Kindman, L. A. (1996) *Proc. Natl. Acad. Sci. USA* **93**, 1993–1996.
34. Mathes, C., Fleig, A. & Penner, R. (1998) *J. Biol. Chem.* **273**, 25020–25030.
35. Tornquist, K., Malm, A. M., Pasternack, M., Kronqvist, R., Bjorklund, S., Tuominen, R. & Slotte, J. P. (1999) *J. Biol. Chem.* **274**, 9370–9377.